

# $J/\psi$ production through resolved photon processes at $e^+e^-$ colliders

R.M. Godbole,  
CTS, Indian Institute of Science, Bangalore 560 012,  
D. Indumathi,  
The Institute of Mathematical Sciences, CIT Campus, Chennai 600 113,  
M. Krämer  
Department of Physics and Astronomy, University of Edinburgh,  
Edinburgh, EH9 3JZ, Scotland

## Abstract:

We consider  $J/\psi$  photoproduction in  $e^+e^-$  as well as linear photon colliders. We find that the process is dominated by the resolved photon channel. Both the once-resolved and twice-resolved cross-sections are sensitive to (different combinations of) the colour octet matrix elements. Hence, this may be a good testing ground for colour octet contributions in NRQCD. On the other hand, the once-resolved  $J/\psi$  production cross-section, particularly in a linear photon collider, is sensitive to the gluon content of the photon. Hence these cross-sections can be used to determine the parton distribution functions, especially the gluon distribution, in a photon, if the colour octet matrix elements are known.

## 1 Introduction

There has been considerable interest in the production of  $J/\psi$  at various colliders ever since the large discrepancy between the measured rate of  $J/\psi$  production and the (much smaller) prediction of the colour singlet (CS) model was first observed at the  $p\bar{p}$  collider Tevatron [1]. An analysis of the data [2] using the NRQCD factorisation approach by Bodwin, Braaten and Lepage [3] yielded colour octet (CO) contributions which seemed almost an order of magnitude larger than the CS term. However, later data from the  $ep$  collider HERA [4] did not see the anticipated excess, especially at large  $z$  values (where  $z$  is the inelasticity variable). Analyses of both fusion [5] and fragmentation [6] contributions to both direct and resolved photon contributions to  $J/\psi$  production at the HERA  $ep$  collider have been performed. In fact, the zero  $p_T$  result has also been evaluated to NLO [7].

The measurement of the  $J/\psi$  and  $\psi(2S)$  polarisation at the Tevatron [8] also did not show the expected large polarisation with increasing  $p_T$  as predicted by NRQCD with a dominant colour octet contribution [9, 10].

This may be attributed to the larger uncertainty of the nonperturbative colour octet matrix elements  $\langle 0|\mathcal{O}^{J/\psi}[n]|0\rangle$ , that contribute in the large- $z$  region. More

recently, it has been proposed [11] that inclusion of the nonvanishing transverse momenta of the colliding partons may drastically change the cross-section, especially at large transverse momenta. In particular, calculations in NRQCD are usually based on collinear factorisation. On including the  $k_{\perp}$  effects, it is possible to fit the octet matrix element  $\langle O^{J/\psi}[8, {}^3S_1] \rangle$  to a much smaller value [12] than that from NRQCD in the collinear limit. This term contributed most substantially to the  $J/\psi$  polarisation; hence this may resolve the problem of the observed  $J/\psi$  polarisation at the Tevatron [12]. However, the discrepancy between the CO fits to the hadroproduction (Tevatron) and leptonproduction (HERA) data remains. It is therefore interesting to estimate the CO as well as CS contributions to  $J/\psi$  production in various other processes.

Here, we examine the dependence of CO  $J/\psi$  photoproduction on the various NRQCD matrix elements in  $e^+e^-$  and photon-photon colliders. (Prompt production at  $e^+e^-$  colliders has been studied in Ref. [13]). Apart from the direct contribution, there are contributions from diagrams where either one or both of the photons is resolved, so that the underlying parton structure is probed. We are concerned here with these resolved photon contributions, the direct contribution being small, as has already been observed for the case of  $\gamma\gamma$  colliders [14, 15].

In particular, there are both colour singlet (CS) and colour octet (CO) contributions to each of these processes. The CS cross section is well known [16]; in fact, it has long since been established that the once resolved (1-res) photon contribution dominates the twice resolved (2-res) photon contribution in the CS case; this was in fact used to estimate the gluon content of the photon [17]. The 1-res case is similar to leptonproduction while the 2-res case is analogous to hadroproduction in  $p\bar{p}$  collisions; hence it will be possible to examine both kinds of processes in a single experiment. Also, effects of intrinsic  $k_{\perp}$  should be different in  $\gamma\gamma$  scattering as compared to  $ep$  or  $p\bar{p}$  processes. In the context of the currently discussed  $k_{\perp}$  factorisation as the solution to the observed  $J/\psi$  polarisation at the Tevatron, it would therefore be interesting to study  $J/\psi$  production in these  $\gamma\gamma$  processes.

These resolved processes have a very different topology from that of the direct processes; hence they can be easily identified. For instance, resolved photon processes have an extra (spectator) jet occurring when a coloured parton of the photon interacts directly in the hard scattering rather than the colour singlet photon itself. Usually this jet is in the same direction as the parent photon (or electron); indeed, it is analogous to the forward jet of remnants produced from deep inelastic scattering off a hadron target. A twice-resolved process, where both the photons are resolved into their parton components will thus have two such jets. Hence direct, 1-res and 2-res processes can be separated event by event, based on the observed topology.

The matrix elements in the CO case, with  $n = [8, {}^3S_1], [8, {}^1S_0],$  and  $[8, {}^3P_J], J = 0, 1, 2,$  are not as well established as the CS ones and have been obtained from  $J/\psi$  production at the Tevatron [2, 18, 19]. Though these are estimated to be about two orders of magnitude smaller than the CS matrix element, the CO contributions are not expected to be small since they correspond to diagrams of lower order in the strong coupling  $\alpha_s$ , or are enhanced by  $t$ -channel gluon exchange, forbidden in the leading-order colour singlet cross section.

We shall therefore compute the CS and CO contributions to the  $J/\psi$  photoproduction cross-section at photon-photon colliders, using certain reasonable estimates

for the corresponding matrix elements. In the next section, we will define the choice of kinematics and list the various subprocesses that contribute to  $J/\psi$  production at an  $e^+e^-$  collider. Numerical results for the cross-section at LEP2 as well as a future possible linear collider at  $\sqrt{s} = 500$  GeV are presented in Section 3. Section 4 discusses the contrasting results obtained for a photon linear collider, where high intensity photon beams can be obtained by scattering laser beams off electron beams. Numerical results here are presented for the case  $\sqrt{s} = 500$  GeV, along with some discussions.

## 2 $J/\psi$ photoproduction in $e^+e^-$ colliders

### 2.1 Kinematics and cross-sections

$J/\psi$  can be produced via direct  $\gamma\gamma$  interaction, or when either or both of the photons are resolved into their partonic constituents. We will refer to the direct interaction, and the once- and twice- resolved photon processes as Direct, 1-res and 2-res processes respectively. Both colour singlet (CS) and colour octet (CO) subprocesses contribute to  $J/\psi$  production in these three channels. Also,  $2 \rightarrow 2$  as well as  $2 \rightarrow 1$  subprocesses contribute. Specifically, they are

Direct:

$$\begin{aligned}\gamma\gamma &\rightarrow (c\bar{c})\gamma \text{ (CS) ,} \\ \gamma\gamma &\rightarrow (c\bar{c})g \text{ (CO) .}\end{aligned}\tag{1}$$

1-res:

$$\begin{aligned}\gamma g_\gamma &\rightarrow (c\bar{c}) \text{ (CO) ,} \\ \gamma g_\gamma &\rightarrow (c\bar{c})g \text{ (CS, CO) ,} \\ \gamma q_\gamma &\rightarrow (c\bar{c})q \text{ (CO) .}\end{aligned}\tag{2}$$

2-res:

$$\begin{aligned}g_\gamma g_\gamma &\rightarrow (c\bar{c}) \text{ (CO) ,} \\ q_\gamma \bar{q}_\gamma &\rightarrow (c\bar{c}) \text{ (CO) ,} \\ g_\gamma g_\gamma &\rightarrow (c\bar{c})g \text{ (CS, CO) ,} \\ g_\gamma q_\gamma &\rightarrow (c\bar{c})g \text{ (CO) ,} \\ q_\gamma \bar{q}_\gamma &\rightarrow (c\bar{c})g \text{ (CO) .}\end{aligned}\tag{3}$$

Note that the zero  $p_T$   $2 \rightarrow 1$  contributions are purely CO. The 1-res processes are analogous to those contributing to the  $ep$  or  $\gamma p$   $J/\psi$  production processes at HERA, while the 2-res ones are analogous to either the resolved  $J/\psi$  photoproduction processes at HERA or to  $J/\psi$  production at the Tevatron. In both cases, the parton densities in the proton are replaced by parton densities in the photon for the case

of interest. Hence modulo the difference in parton densities, the production rate in the 1-res channel should reflect that seen at HERA and the 2-res channel that at Tevatron. The  $J/\psi$  production data from  $e^+e^-$  collisions can therefore provide a corroboration of the behaviour seen at  $ep$  and  $p\bar{p}$  colliders, and establish whether there is indeed a dominant CO contribution in  $J/\psi$  production at colliders.

The cross-section in the CM frame for the process  $e^+e^- \rightarrow J/\psi X$  is given by

$$\frac{d^3\sigma}{dx_1 dx_2 d\hat{t}} = p_1(x_1)p_2(x_2)\frac{d\hat{\sigma}}{d\hat{t}} + (x_1 \leftrightarrow x_2) ,$$

where 1 and 2 refer to the  $e^+$  and  $e^-$  respectively. Here  $p_e(x)$  corresponds to  $\gamma_e(x)$  for the case of the unresolved photon and equals the convolution,

$$p_e(x) = \int_x^1 \frac{dy}{y} \gamma_e(y) p_\gamma(x/y) ,$$

in terms of the parton density  $p_\gamma(x)$ ,  $p = q, g$ , in the resolved photon. We use the Weizäcker-Williams approximation (WWa) for the bremsstrahlung photon distribution from an electron:

$$f_{\gamma_e}(z) = \frac{\alpha_{\text{em}}}{2\pi} \left( \frac{1 + (1-z)^2}{z} \log(q_{\text{max}}^2/q_{\text{min}}^2) + 2m_e^2 z \left( \frac{1}{q_{\text{max}}^2} - \frac{1}{q_{\text{min}}^2} \right) \right) , \quad (4)$$

where  $q_{\text{min}}^2 = m_e^2 z^2/(1-z)$  and  $q_{\text{max}}^2 = (E\theta)^2(1-z) + q_{\text{min}}^2$ . Here  $z = E_\gamma/E_e$ ,  $\theta$  is the angular cut that ensures the photon is real, and  $E = E_e = \sqrt{s}/2$ . We use a typical value of  $\theta = 0.03$  in our analysis. for  $\sqrt{s} = 175$  GeV.

### 3 Numerical results

We recast the cross-section in terms of the hadronic variables,  $y_1$ ,  $y_2$  and  $p_T$  and compute the  $p_T$  dependence of the cross-section:

$$\frac{d\sigma}{dp_T}(e^+e^- \rightarrow e^+e^- J/\psi X) .$$

We use a common renormalisation and factorisation scale,  $q^2 = (m_c^2 + p_T^2)$  with  $m_c = 1.5$  GeV and  $\Lambda_{\text{QCD}}^4 = 200$  MeV. We use the GRV leading order (LO) parametrisation [20] for the parton densities inside the photon. Similar results are obtained on using the WHIT parametrisation [21] instead.

We shall use the following reasonable choices for the matrix elements which are consistent with the allowed values:  $\langle O^{J/\psi}[1, {}^3S_1] \rangle = 1.16$  GeV<sup>3</sup>,  $\langle O^{J/\psi}[8, {}^3S_1] \rangle = 10^{-2}$  GeV<sup>3</sup>,  $\langle O^{J/\psi}[8, {}^1S_0] \rangle = 10^{-2}$  GeV<sup>3</sup>,  $\langle O^{J/\psi}[8, {}^3P_0] \rangle/m_c^2 = 10^{-2}$  GeV<sup>3</sup>, where the remaining  $J$  values are fixed from symmetry:  $\langle O^{J/\psi}[8, {}^3P_J] \rangle = (2J+1)\langle O^{J/\psi}[8, {}^3P_0] \rangle$ .

We compute the  $p_T$  dependence of the cross-section for the direct  $\gamma\gamma$ , the 1-res photon and the 2-res photon cases. The CS and CO cross-sections,  $d\hat{\sigma}/d\hat{t}$ , for all the processes listed in eqs. (1-3) are known [14, 22, 23]. The results for the direct case are shown in Fig. 1, where the differential cross-section for the direct  $\gamma\gamma$  interaction [14] is plotted as a function of  $p_T$ . The  $[8, {}^3S_1]$  octet matrix element that occurs here does not contribute dominantly to this cross-section.

For the 1-res case, there are contributions from the  ${}^3S_1$ ,  ${}^1S_0$  and  ${}^3P_J$  octet matrix elements apart from the singlet  ${}^3S_1$  term [22]. The  $\gamma g$  interaction term is expected to dominate this cross-section. These are shown as dashed lines in Fig. 2, where the individual contributions are shown. The slope ( $p_T$  dependence) of the octet  $[8, {}^1S_0]$  and  $[8, {}^3P_J]$  terms is very similar with the ratio of the two contributions ranging from about 0.15 near  $p_T = 1$  GeV to about 0.32 near  $p_T = 15$  GeV for  $m_c = 1.5$  GeV. The slopes of the singlet and octet  ${}^3S_1$  terms are very different from these. Hence it may be possible to separate the contribution involving the combination of matrix elements ( $\langle O^{J/\psi}[8, {}^1S_0] \rangle + 7\langle O^{J/\psi}[8, {}^3P_J] \rangle / m_c^2$ ) from that of the  ${}^3S_1$  terms, at small  $p_T$ . (At larger  $p_T$ , the cross-section drops off rapidly).

A note about the cross-section as  $p_T \rightarrow 0$ . While the direct cross-section remains finite for  $p_T \rightarrow 0$ , only the  ${}^3S_1$  singlet and octet terms are finite for the 1-res case. The  $2 \rightarrow 2$  processes involving the  ${}^1S_0$  and  ${}^3P_J$  terms diverge in the small- $p_T$  limit. However, precisely these processes have a finite CO contribution from the  $2 \rightarrow 1$  zero  $p_T$  processes; in fact, these  $2 \rightarrow 2$   $\gamma g \rightarrow (c\bar{c})g$  processes at  $p_T \rightarrow 0$  are just these  $2 \rightarrow 1$  processes with a soft gluon emission. The apparent divergence of the  $2 \rightarrow 2$  cross-section at  $p_T \rightarrow 0$  can be resummed into a finite correction to the  $2 \rightarrow 1$  lower order process ( $K$ -factor) [7]. Hence the  $p_T = 0$  cross-section for the  $[8, {}^1S_0]$  and  $[8, {}^3P_J]$  processes is within a  $K$ -factor of the corresponding  $2 \rightarrow 1$  cross-section<sup>1</sup> which is indicated by the arrows marked in Fig. 2.

Finally, the effect of including the  $\gamma q$  terms is shown by the solid lines in Fig. 2. The quark contribution increases with  $p_T$  and is small. The one exception is the  $[8, {}^3S_1]$  contribution which is significantly enhanced by inclusion of the quark diagrams; however, this may still not be large enough to be observable. The  $\gamma q$  cross-section also diverges at small  $p_T$ . Here there is no corresponding  $2 \rightarrow 1$  lower order process. However, the  $J/\psi$  here is produced by fragmentation of a gluon; the soft divergence at  $p_T = 0$  must therefore be absorbed into the fragmentation function in this case.

The subprocess cross-sections for 2-res processes are the same as those for  $p\bar{p}$  collisions [23] since the parton content of both photons is resolved in this case. Contributions are from  $gg$ ,  $gq$  and  $q\bar{q}$  subprocesses. Here it turns out that the octet  $[8, {}^3S_1]$  term dominates at large  $p_T$  as can be seen from Fig. 3. The  $[8, {}^1S_0]$  and the  $[8, {}^3P_J]$  terms dominate at low  $p_T$  and contribute in the same ratio as in the 1-res case. Notice that the ( $\langle O^{J/\psi}[8, {}^1S_0] \rangle + 7\langle O^{J/\psi}[8, {}^3P_J] \rangle / m_c^2$ ) contribution is much larger than the CS term, unlike in the 1-res case. Hence, even if the octet matrix elements are overestimated by a factor of 10, the CO contribution is still substantial in the 2-res case. Note also that, while the 2-res cross-section is only a few percent of the 1-res one, it can be kinematically easily distinguished from the 1-res case and can be analysed for its CO content. Hence it may be possible to determine these CO matrix elements accurately through the 2-res channel. As in the 1-res case, the arrows in Fig. 3 at  $p_T = 0$  indicate the  $2 \rightarrow 1$  contribution from the octet  $[8, {}^3S_1]$ ,  $[8, {}^1S_0]$  and  $[8, {}^3P_J]$  terms. The actual  $p_T = 0$  cross-section will be within a  $K$ -factor of this (from the soft limit of the corresponding  $2 \rightarrow 2$  diagrams). The CS term is finite as  $p_T \rightarrow 0$ , as in the 1-res case. At a collider, it may be possible to observe the zero  $p_T$   $J/\psi$ 's by

---

<sup>1</sup>The  $2 \rightarrow 1$  cross-sections shown in Fig. 2 of Ref. [24] should have been multiplied by the corresponding matrix elements, that is, by a factor of  $10^{-2}$ . Hence the conclusion drawn in that article about a substantial  $2 \rightarrow 1$  contribution at zero  $p_T$  is wrong.

reconstructing the leptonic decay mode.

There exists substantial amount of data from LEP at  $\sqrt{s} = 189$  GeV as well; the results in this case are very similar to what is obtained at the slightly smaller value of  $\sqrt{s}$  used here. The variation of the cross-section with the CM energy is shown in the next two figures. The total 1-res cross-section (integrated from  $p_{T,\min} = 1$  GeV to a kinematical maximum of  $p_{T,\max} = \sqrt{s}/2$ ) is shown in Fig. 4 as a function of the centre of mass energy,  $\sqrt{s}$ . The cross-section is small at lower energies, as are available at colliders such as TRISTAN but increases with  $\sqrt{s}$ . The cross-section at an  $e^+ e^-$  collider with  $\sqrt{s} = 500$  GeV is  $\sigma(P_{T,\min} = 1 \text{ GeV}) = 68$  pb. The number of  $J/\psi$ s seen will depend on the luminosity, and the branching fraction of the cleanest decay mode,  $J/\psi \rightarrow l^+ l^-$ , which is 6%. However the ratio of the octet  $[8, {}^1S_0]$  to  $[8, {}^3P_J]$  terms is a fairly steady 0.15 over a large range of  $\sqrt{s}$ . Hence it is possible that a combination of 1-res and 2-res processes at  $e^+ e^-$  colliders can help determine the universal CO matrix elements occurring in  $J/\psi$  production.

The corresponding total cross-section for the 2-res case is plotted in Fig. 5. In general, the inclusion of CO terms does not affect the result that the 1-res dominates the 2-res contributions. Also, we find that the CO contribution is much larger than the CS one; this may also reflect the fact that we have used octet matrix elements from the Tevatron fits which may overestimate  $J/\psi$  production at HERA. However, independently of this, the 1-res contribution dominates. This is in contrast to the  $e-p$  case, for example, at HERA, where the resolved photon contribution (corresponding to the 2-res term in  $\gamma\gamma$  collisions) is an appreciable fraction of the direct one (corresponding to the 1-res term of  $\gamma\gamma$  collisions) [25, 26].

Realistic acceptance cuts on the lepton angle and  $p_T$  should reduce the event rates at TRISTAN by approximately a factor two but only by about 10% in the case of LEP2. Accurate estimates will be presented in a future work.

In the case of larger  $p_T$  events, the situation is not so promising, since the production rate falls very rapidly with  $p_T$ . What may be interesting to examine is whether rapidity cuts will enhance the colour octet contribution or else distinguish in some way the CO from the CS part. We leave this question to future work.

Finally, we remark that there is a further uncertainty in  $e^+ e^-$  collisions compared to  $e-p$  collisions since the parton densities in the photon are not as well known as those in the proton.

The dependence of the cross-section on the choice of parametrisation is shown in Fig. 6. The four panels show the sensitivity of the individual gluon contribution only for the different 1-res singlet and CO contributions when the WHIT rather than the GRV parametrisations are used. The WHIT1 gluon is closest to the GRV gluon. The WHIT2,3 are smaller at  $x > 0.1$  while the WHIT4 has a gluon that is twice that of WHIT1. While the corrections are rather large, especially for the WHIT4 density, where it exceeds 50%, the  $p_T$  dependence is the same (in all 4 panels) for a given parametrisation for all the CS and CO terms and is rather flat. Unless the CS and CO matrix elements are known to precision, therefore, it may not be possible to distinguish the different parametrisations from the 1-res cross-section.

This can be seen from Fig. 7 where the 1-res and 2-res cross-sections are shown for a future linear collider at  $\sqrt{s} = 500$  GeV. The total cross-section is about an order of magnitude larger than at LEP2; however, the other features (such as the  $p_T$  dependence of the various CS and CO contributions) remain the same when we go to

larger  $\sqrt{s}$  values. The sensitivity of the cross-section to the choice of parton densities in a photon is also shown in this figure. There is not much difference between the predictions from the GRV [20] and WHIT4 [21] parton distribution sets for the 1-res case. However, since both photons are resolved into their partonic content in the 2-res case, the predictions are more sensitive to the densities in the 2-res case. It is seen that the cross-sections are systematically higher when the WHIT4 parametrisation is used than with the GRV set. However, the shape ( $p_T$  dependence) remains roughly the same, independent of choice of parametrisation.

## 4 $J/\psi$ production from a photon linear collider

High intensity photon beams can be obtained by back-scattering of laser beams off electron beams. Such a photon linear collider can have high energies of  $\sqrt{s} = 500$ – $1000$  GeV and very high luminosity. Hence there has recently been a great deal of interest in such colliders.

The  $J/\psi$  production processes here are the same as in  $e^+e^-$  colliders. Since the photons are accelerated by back-scattering, they are distributed very differently from the WWa case. In place of eq. (4) for the WWa photons, we have

$$\gamma_{\text{laser}}(z) = \left( \frac{1}{1-z} + 1 - z - 4r(1-r) \right) \frac{1}{\sigma_c}, \quad (5)$$

where  $r = z/(\kappa(1-z))$  and the maximum energy of the photon is limited to  $z_{\text{max}} = \kappa/(1+\kappa)$ , where the dimensionless variable,  $\kappa$ , is given by,

$$\kappa = \frac{4E_b E_0}{m_e^2} \cos \theta/2,$$

for an electron beam of energy  $E_b$ , a laser of energy  $E_0$  and  $\theta$  the angle between them. Here,

$$\sigma_c = \log(1+\kappa) + z_{\text{max}}^2 \left( \frac{\kappa+2}{2\kappa} \right) + \frac{4}{\kappa} (z_{\text{max}} + \kappa - 2 \log(1+\kappa)),$$

and we choose  $\kappa = 4.83$  to avoid background from pair creation processes,  $\gamma\gamma \rightarrow e^+e^-$ , in the collision.

We again use the GRV parametrisation [20] for parton distributions in the photon and compute the same cross-section, but for the laser back-scattered photon-photon scattering. That is, the subprocesses are the same as for the  $e^+e^-$  case, but the laser photon distribution given in eq. (5) is to be used instead of the WWa distribution. We present the results for such a future collider with  $\sqrt{s} = 500$  GeV in Figs. 8, 9, 10. Since the subprocesses are the same as in the  $e^+e^-$  case, the  $p_T$  dependences are the same as before, with the same behaviour of the octet  $[8, ^1S_0]$  and  $[8, ^3P_J]$  terms. The advantage here is in the event rate which is much larger than in  $e^+e^-$  colliders, as can be seen from the much larger cross-section in this case. Furthermore, the direct contribution in photon colliders is much smaller (by about two orders of magnitude) than in  $e^+e^-$  colliders. Hence  $J/\psi$  production at photon colliders will be dominated by the resolved contributions. Photon colliders will therefore be good sites for testing the colour octet contribution and obtaining the octet matrix elements that occur in  $J/\psi$  production. Furthermore, the quark contribution to the 1-res case is negligible here. Hence the 1-res cross-section is proportional to the gluon content of the photon.

We have ignored the contribution to the cross-section from  $\chi$  feed-down; however, with sufficient data, it may be possible to separate the prompt  $J/\psi$  production rate from these decay modes. It may still be hard to separate out the individual octet  $[8, ^1S_0]$  and  $[8, ^3P_J]$  contributions in these processes.

In conclusion,  $J/\psi$  photoproduction at both  $e^+ e^-$  as well as photon linear colliders can prove to be a sensitive testing ground to determine the colour octet contribution in  $J/\psi$  production. This, in comparison with the data from  $p\bar{p}$  and  $ep$  colliders, can help determine the colour octet matrix elements involved in  $J/\psi$  production. It is also possible to use the shape of the  $p_T$  spectrum to determine the various contributions. Turning the problem around, if the NRQCD matrix elements for the process are determined by other experiments, it is possible to use the measured  $J/\psi$  photoproduction cross-sections as proposed in this paper, to determine the parton distribution functions in a resolved photon.

**Acknowledgement** : MK thanks M. Cacciari, B.A. Kniehl and F. Maltoni for useful discussions. The work of RMG and DI was supported in part under CSIR grant No. 3 (745) 94-EMR-II. The authors also wish to thank the DST and the organisers of the fifth Workshop on High Energy Phenomenology (WHEPP-5), where these results were first presented.

## References

- [1] CDF Collaboration, F. Abe et al., Phys. Rev. Lett. 75 (1995) 4358 and *ibid.* 79 (1997) 578.
- [2] P. Cho and A.K. Leibovich, Phys. Rev. D53 (1996) 150; *ibid.*, (1996) 6203.
- [3] G.T. Bodwin, E. Braaten, G.P. Lepage, Phys. Rev. D51 (1995) 1125 (erratum: *ibid.* D55 (1997) 5853).
- [4] H1 Collaboration, S. Aid et al., Nucl. Phys. B472 (1996) 3; ZEUS Collaboration, J. Breitweg et al., Z. Phys. C75 (1997) 215.
- [5] M. Cacciari and M. Krämer, Phys. Rev. Lett. 76 (1996) 4128; P. Ko, J. Lee, and H.S. Song, Phys. Rev. D54 (1996) 4312, Erratum *ibid.* **D60** (1999) 119902; updated version in preprint hep-ph/9602223.
- [6] B.A. Kniehl and G. Kramer, Phys. Rev. **D 56** (1997) 5820.
- [7] A. Petrelli, M. Cacciari, M. Greco, F. Maltoni, M.L. Mangano, Nucl. Phys. **B 514** (1998) 245; F. Maltoni, M.L. Mangano and A. Petrelli, Nucl. Phys. **B 519** (1998) 361.
- [8] The CDF Collab., T. Affolder et al., Fermilab publication FERMILAB-PUB-00/090-E, hep-ex0004027, to appear in Phys. Rev. Lett. 2000.
- [9] M. Beneke and M. Krämer, Phys. Rev. **D 55** (1997) 5629; A.K. Leibovich, Phys. Rev. **D 56** (1997) 4412.
- [10] E. Braaten, B. Kniehl and J. Lee, Phys. Rev. **D 62** (2000) 094005.



- [11] Ph. Hägler, R. Kirschner, A. Schäfer, L. Szymanowski and O.V. Teryaev, hep-ph/0004263, 2000.
- [12] Ph. Hägler, R. Kirschner, A. Schäfer, L. Szymanowski and O.V. Teryaev, hep-ph/0008316, 2000; F. Yuan and K.-Ta. Chao, hep-ph/0009224, 2000.
- [13] F. Yuan, C.-F. Qiao, and K.-Ta. Chao, Phys. Rev. **D 56** (1997) 321. C. Glenn Boyd, A.K. Leibovich, and I.Z. Rothstein, Phys. Rev. **D 59** (1999) 054016.
- [14] J.P. Ma, B.H.J. McKellar, and C.B. Paranaavitane, Phys. Rev. **D 57** (1998) 606 [hep-ph/9707480]. The results in this paper differ from that of Japaridze and Tkabladze in ref. [15] above (note that the definitions of the CO and CS contributions have been interchanged here) for the CS contribution by a factor of 3/4. We agree with the results given in the paper by Ma, McKellar and Paranaavitane, which have also been obtained by M. Klasen, B.A. Kniehl, L. Mihaila and M. Steinhauser, Nucl. Phys. **B 609** (2001) 518 [hep-ph/0104044]. There is agreement between our analysis and that of Figure 4 of Klasen et al. See also the related work of C.F. Qiao, preprint hep-ph/0104309, to appear in Phys. Rev. **D**.
- [15] G. Japaridze and A. Tkabladze, Phys. Lett. **B 433** (1998) 139 [hep-ph/9803447]. 1998.
- [16] R. Baier and R. Rückl, Nucl. Phys. B201 (1982) 1 and Z. Phys.. C19 (1983) 251.
- [17] M. Drees and R.M. Godbole, J. Phys. G21 (1995) 1559.
- [18] M.A. Sanchis-Lozano, Nucl. Phys. Proc. Suppl. **86** (2000) 543.
- [19] Adam K. Leibovich, preprint hep-ph/0008236, talk given at the 4th Int. conference on hyperons, charm and beauty hadrons, Valencia, Spain, 27-30 Jun, 2000.
- [20] M. Glück, E. Reya, A. Vogt, Phys. Rev. D46 (1992) 1973.
- [21] K. Hagiwara, M. Tanaka, I. Watanabe, and T. Izubuchi, Phys. Rev. D51 (1995) 3197.
- [22] E.L. Berger and D. Jones, Phys. Rev. **D 23** (1981) 1521 (for the CS part). For the CO cross-section, see the references listed in ref. [5].
- [23] For the CS part, see R. Baier and R. Rückl in ref. [16]; R. Gastmans, W. Troost and T.T. Wu, Phys. Lett. **B 184** (1987) 257; Nucl. Phys. **B 291** (1987) 731. For the CO cross-section, see the reference to P. Cho and A.K. Leibovich in ref. [2] above.
- [24] R.M. Godbole, D. Indumathi and M. Krämer, in Proceedings of the 5th Workshop on high energy physics phenomenology (WHEPP5), Pune, January 1998, Pramana, J. Phys. **51** (1998) 301.
- [25] M. Cacciari and M. Krämer, in Proceedings of the Workshop on Future Physics at HERA, hep-ph/9609500.

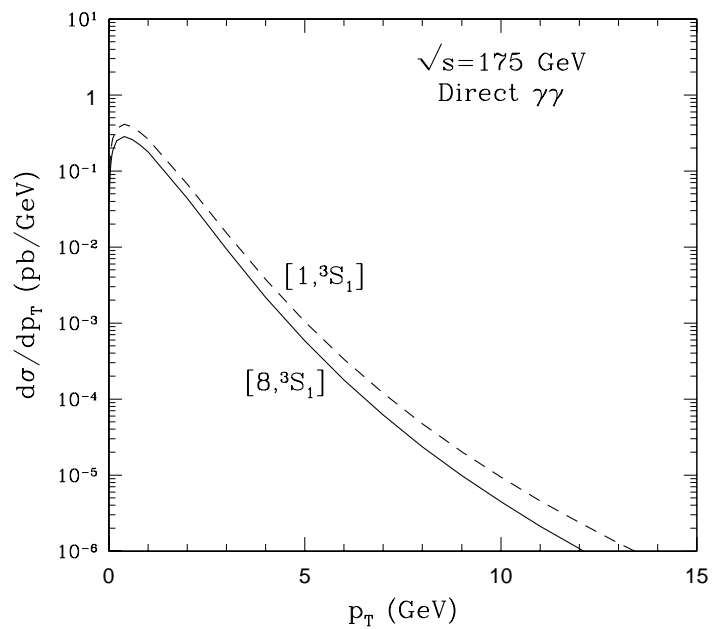


Figure 1: The direct  $J/\psi$  photoproduction cross-section at LEP2 is shown as a function of  $p_T$ . The CS and CO contributions are separately shown.

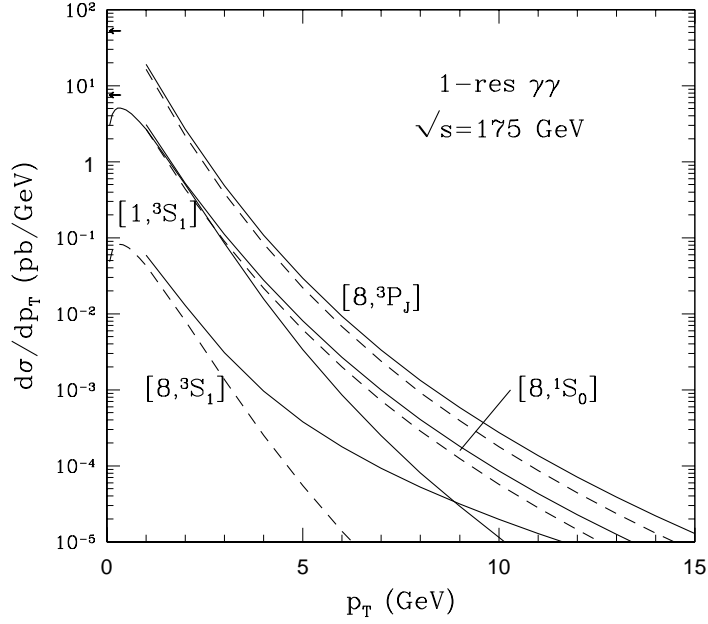


Figure 2: The  $J/\psi$  photoproduction cross-section from once-resolved (1-res) processes at LEP2 is shown as a function of  $p_T$ . The CS and CO contributions are separately shown. The dashed (solid) lines correspond to the gluon (total) CO cross-sections, the two differing substantially only for the  $^3S_1$  case. The arrows indicate the zero  $p_T$   $[8, ^3P_J]$  and  $[8, ^1S_0]$  cross-sections (in pb), arising from the corresponding  $2 \rightarrow 1$  subprocesses.

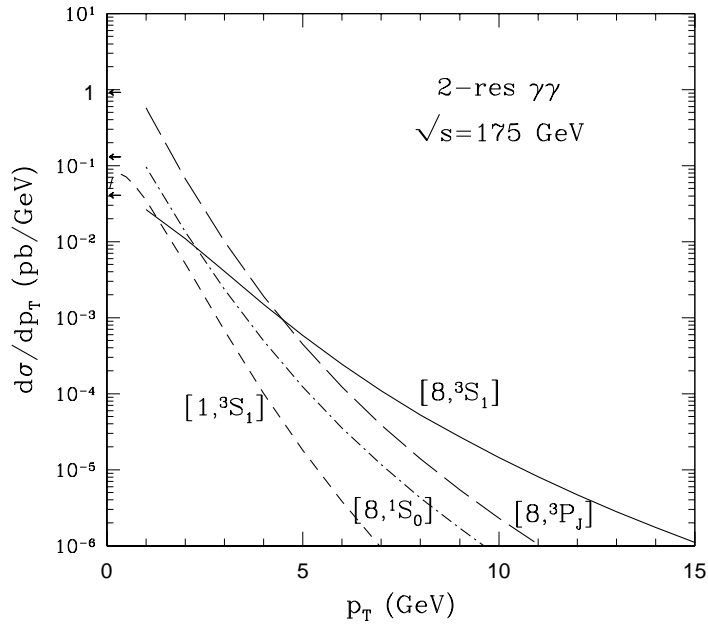


Figure 3: The  $J/\psi$  photoproduction cross-section from twice-resolved (2-res) processes at LEP2 is shown as a function of  $p_T$ . The CS and CO contributions are separately shown. The arrows indicate the zero  $p_T$   $[8, ^3P_J]$ ,  $[8, ^1S_0]$  and  $[8, ^3S_1]$  cross-sections (in pb), arising from the corresponding  $2 \rightarrow 1$  subprocesses.

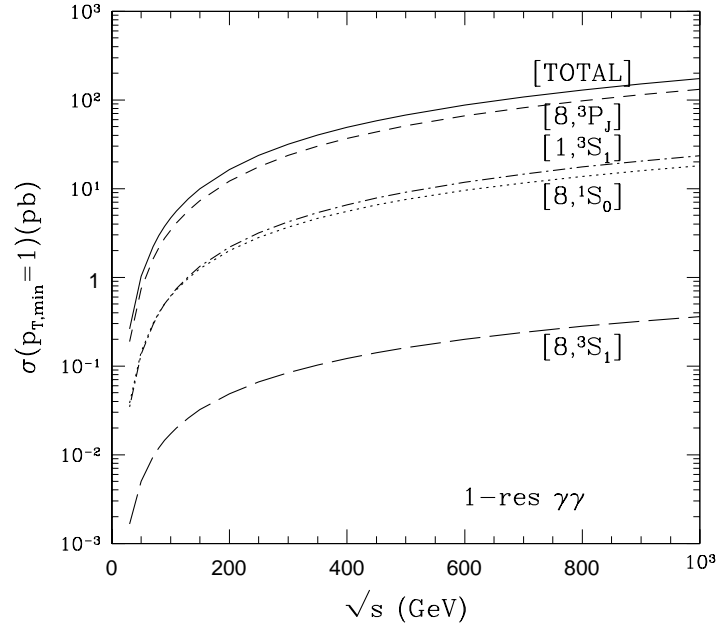


Figure 4: The 1-res  $J/\psi$  photoproduction cross-section integrated over  $p_T$  from  $p_{T,\min} = 1$  GeV, shown as a function of  $\sqrt{s}$ . The CS, CO and total contributions are separately shown.

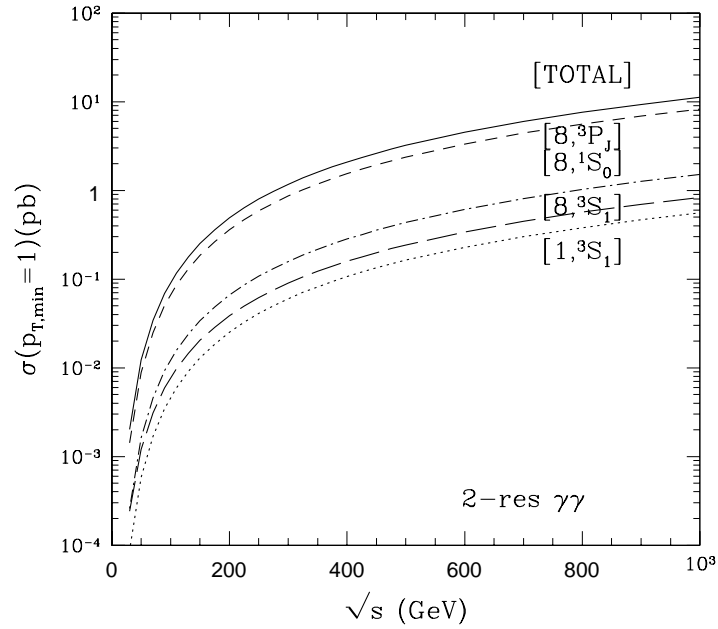


Figure 5: As in Fig. 4 for the integrated 1-res cross-section, but for the 2-res case.

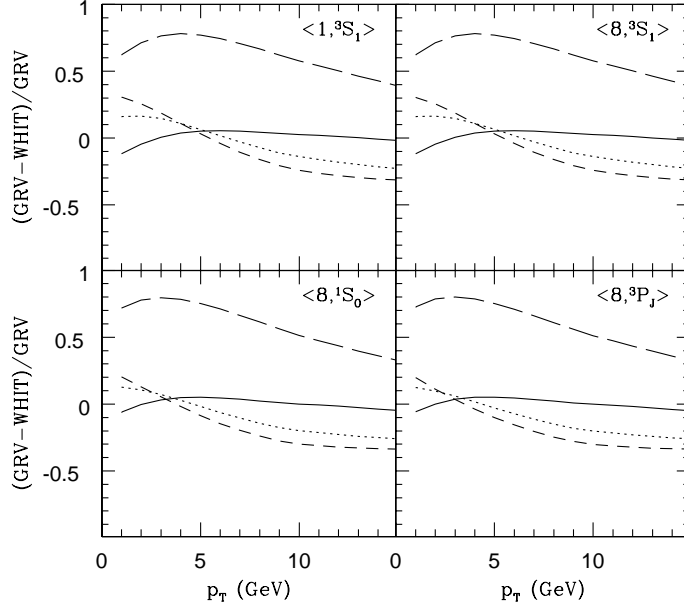


Figure 6: The variation of the  $J/\psi$  photoproduction cross-section from once-resolved (1-res) processes at LEP2 for different parametrisations of the photon density is shown as a function of  $p_T$ . The solid, dotted, dashed and long-dashed lines correspond to the WHIT1,2,3,4 parametrisations for the gluon density.

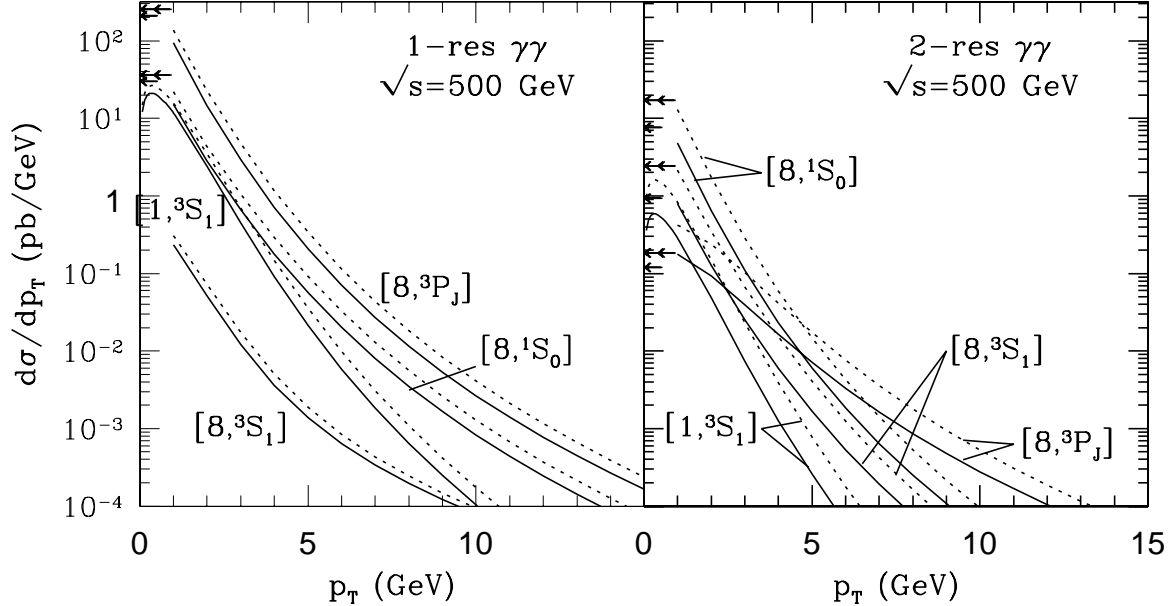


Figure 7: The total CS and CO 1-res and 2-res  $J/\psi$  photoproduction cross-sections shown as a function of  $p_T$  for a future  $e^+e^-$  linear collider at  $\sqrt{s} = 500$  GeV. Solid and dotted lines (correspond to the use of GRV and WHIT4 parametrisations for the parton densities in a photon). The zero  $p_T$   $2 \rightarrow 1$  contributions (in pb) are indicated by (double) arrows for the (WHIT) GRV cases respectively.

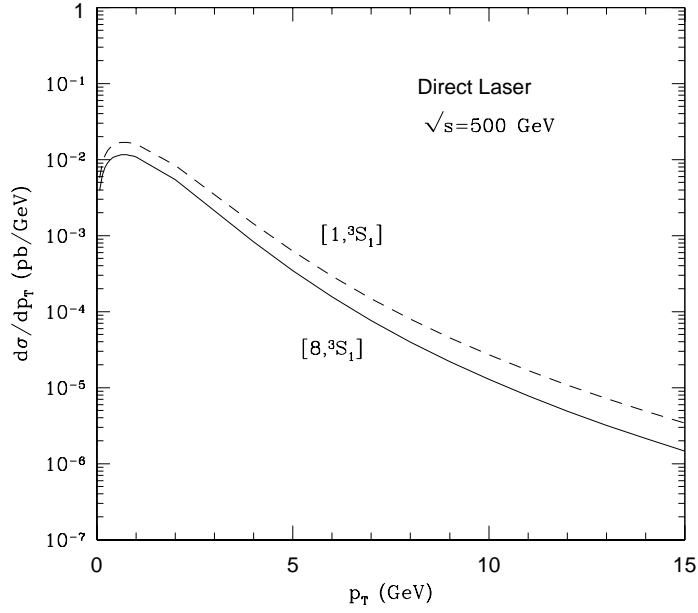


Figure 8: The same as Fig. 1, but for a laser backscattered photon at  $\sqrt{s} = 500$  GeV.

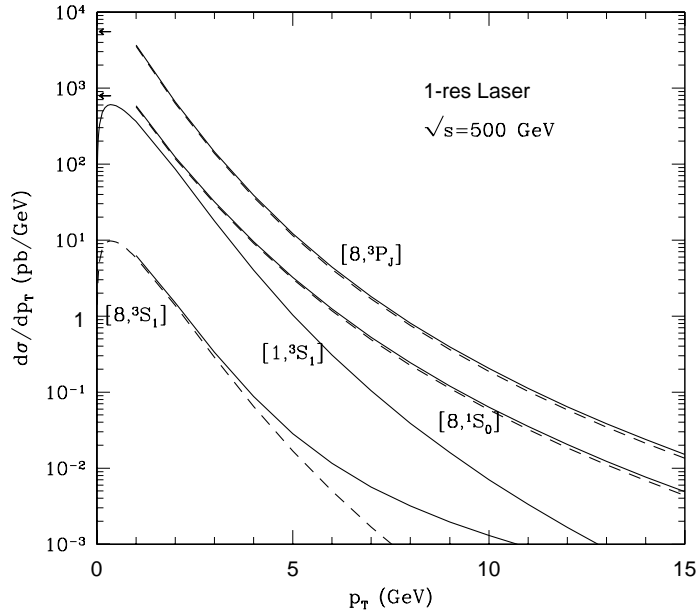


Figure 9: The same as Fig. 2, but for a laser backscattered photon at  $\sqrt{s} = 500$  GeV.

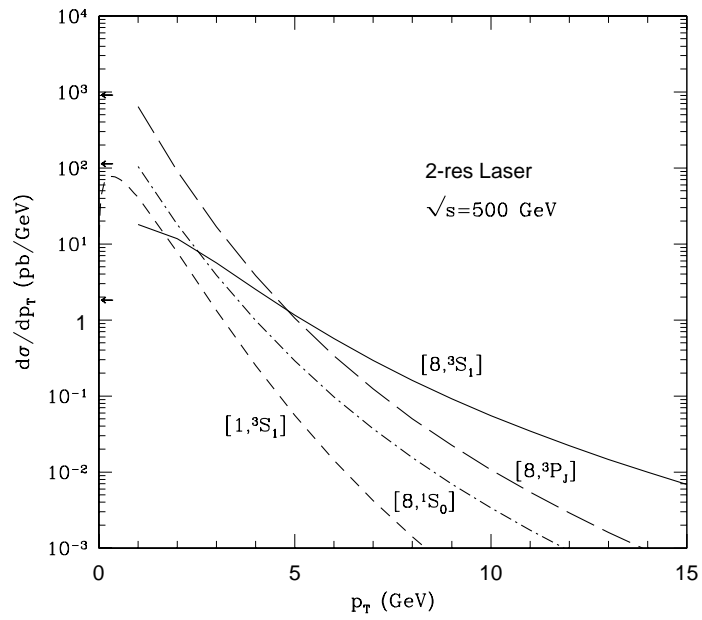


Figure 10: The same as Fig. 3, but for a laser backscattered photon at  $\sqrt{s} = 500$  GeV.